

$$(x - y_R)G_{N,j} - G_{N-1,j} = \delta_{N,j}v, \quad (6)$$

where $j=1, 2, \dots, N$ and $\delta_{i,j}$ is the Kronecker δ . The Green's function G_{jj} can be solved exactly from the above equations as follows:

$$G_{jj}(\omega) = \frac{\Delta(G_{jj})(\omega)}{v \cdot \Delta(G)(\omega)}, \quad (7)$$

where $\Delta(G_{jj})$ is given by

$$\Delta(G_{jj})(\omega) = \begin{cases} (x - y_R)B_{N-2}(x) - B_{N-3}(x), & j = 1 \\ [(x - y_L)B_{j-2}(x) - B_{j-3}(x)][(x - y_R)B_{N-j-1}(x) - B_{N-j-2}(x)], & 2 \leq j \leq N-1 \\ (x - y_L)B_{N-2}(x) - B_{N-3}(x), & j = N. \end{cases} \quad (8)$$

It is worth pointing out that no approximation has been made for the Green's functions: G_{jj} and G_{1N} .

Starting from G_{jj} and G_{1N} , we work out analytically the rigorous expressions for transport properties, such as the dc current, the differential conductance, and the density of states, in an N -coupled quantum dot array.

The dc current. Following the definition of the electronic current^{10,12} and using Eq. (3), the dc current flowing from the left reservoir to the right reservoir is given by

$$J = \frac{4e}{h} \int d\omega [f_L(\omega) - f_R(\omega)] \Delta_L \Delta_R |G_{1N}(\omega + i0)|^2, \quad (9)$$

where $f_\alpha(\omega) = \{\exp[\beta(\omega - \mu_\alpha)] + 1\}^{-1}$ is the Fermi distribution function for the reservoir α , and μ_α is the chemical potential of the reservoir α . Here using the wide-band limit,¹⁰ we have $\sum_k v_{k\alpha}^2 (\omega - \varepsilon_{k\alpha} + i0)^{-1} = -i\Delta_\alpha$, in which Δ_L and Δ_R are the resonant widths associated with the tunneling between the left reservoir and the first dot, and that between the right reservoir and the N th dot, respectively. In the following, we use $\tilde{E} \equiv E/v$ for energy and omit the superscript of wave. In terms of the Green's function G_{1N} , therefore, the dc current can be rewritten as

$$J = \frac{4e}{h} \int d\omega [f_L(\omega) - f_R(\omega)] \frac{\Delta_L \Delta_R}{[\eta^2(\omega) + \xi^2(\omega)]}, \quad (10)$$

where

$$\eta(\omega) = [(\omega - \varepsilon_0)^2 - \Delta_L \Delta_R] B_{N-2}(\omega - \varepsilon_0) - 2(\omega - \varepsilon_0) B_{N-3}(\omega - \varepsilon_0) + B_{N-4}(\omega - \varepsilon_0)$$

and

$$\xi(\omega) = (\Delta_L + \Delta_R)[(\omega - \varepsilon_0)B_{N-2}(\omega - \varepsilon_0) - B_{N-3}(\omega - \varepsilon_0)].$$

The differential conductance. By setting the Fermi level μ_R of the right reservoir fixed ($\mu_R=0$), the differential conductance with respect to the chemical potential μ_L ($\mu_L=\mu$) of the left reservoir can be obtained analytically as follows:

$$\sigma = \frac{4e^2}{h} \int d\omega \left[-\frac{df(\omega - \mu)}{d\omega} \right] \frac{\Delta_L \Delta_R}{[\eta^2(\omega) + \xi^2(\omega)]}. \quad (11)$$

The density of states. According to the definition of the density of states $\rho_j \equiv -\frac{1}{\pi} \text{Im} G_{jj}(\omega + i0)$ and Eq. (7), the density of states of electrons in the j th quantum dot can be given by

$$\rho_j = \frac{1}{\pi} \frac{\xi(\omega)u_j(\omega) - \eta(\omega)w_j(\omega)}{\eta^2(\omega) + \xi^2(\omega)}, \quad (12)$$

where

$$u_j(\omega) = \begin{cases} (\omega - \varepsilon_0)B_{N-2}(\omega - \varepsilon_0) - B_{N-3}(\omega - \varepsilon_0), & j = 1 \\ [(\omega - \varepsilon_0)B_{j-2}(\omega - \varepsilon_0) - B_{j-3}(\omega - \varepsilon_0)][(\omega - \varepsilon_0)B_{N-j-1}(\omega - \varepsilon_0) - B_{N-j-2}(\omega - \varepsilon_0)] \\ - \Delta_L \Delta_R B_{j-2}(\omega - \varepsilon_0) B_{N-j-1}(\omega - \varepsilon_0), & 2 \leq j \leq N-1 \\ (\omega - \varepsilon_0)B_{N-2}(\omega - \varepsilon_0) - B_{N-3}(\omega - \varepsilon_0), & j = N \end{cases}$$

and

$$w_j(\omega) = \begin{cases} \Delta_R B_{N-2}(\omega - \varepsilon_0), & j = 1 \\ \Delta_L B_{j-2}(\omega - \varepsilon_0)[(\omega - \varepsilon_0)B_{N-j-1}(\omega - \varepsilon_0) - B_{N-j-2}(\omega - \varepsilon_0)] + \Delta_R B_{N-j-1}(\omega)[(\omega - \varepsilon_0)B_{j-2}(\omega) - B_{j-3}(\omega)], & 2 \leq j \leq N-1 \\ \Delta_L B_{N-2}(\omega - \varepsilon_0), & j = N \end{cases} .$$

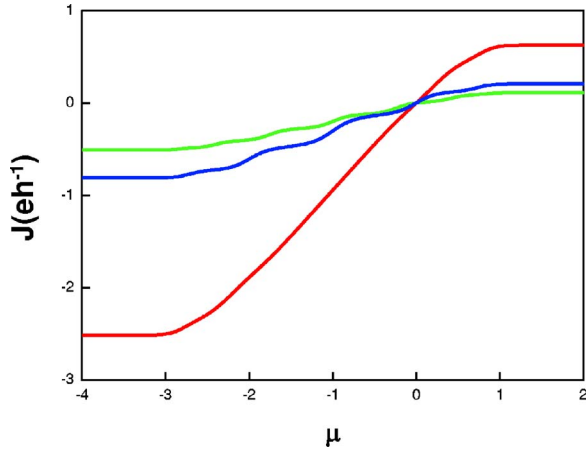


FIG. 1. (Color online) Plot of the dc current against the left Fermi level for $N=7$, $kT=0.08$, and $\varepsilon_0=-1$ at different resonant widths: $\Delta=0.1$ (green), 1.0 (red), 6.0 (blue). All energies are expressed by units of v .

It is a remarkable fact that the exact expressions for the dc current, the differential conductance, and the density of states, have explicitly algebraic structures. For arbitrary dot number N , the resonant widths Δ_L and Δ_R , and the interdot tunnel coupling v , these transport properties can be calculated exactly.

Within the wide-band limit, the resonant widths Δ_L and Δ_R are energy-independent constants, so we take $\Delta_L=\Delta_R=\Delta$ for simplicity. According to the rigorous formulas (10) and (11), we plot the curves for the dc current and the differential conductance with respect to μ . Without losing generality, we consider the quantum dot array of $N=7$.

Figure 1 shows the dependence of the dc current on the bias voltage μ . At low temperatures, the dc current versus μ has a steplike structure when the resonant width Δ , which relates the tunnel coupling between the reservoir and its nearby dot, is much larger or smaller than the tunnel coupling v between the intermediate dots. With increasing the temperature or the number of quantum dots, the dc current

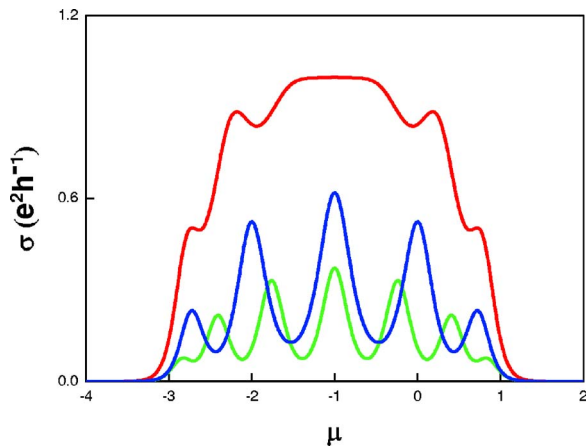
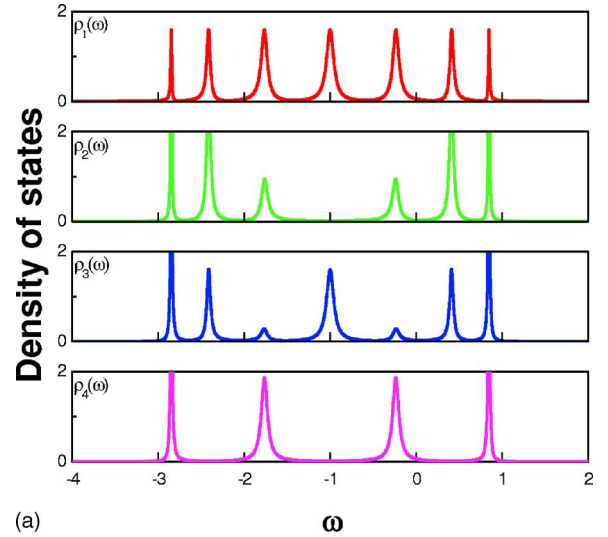
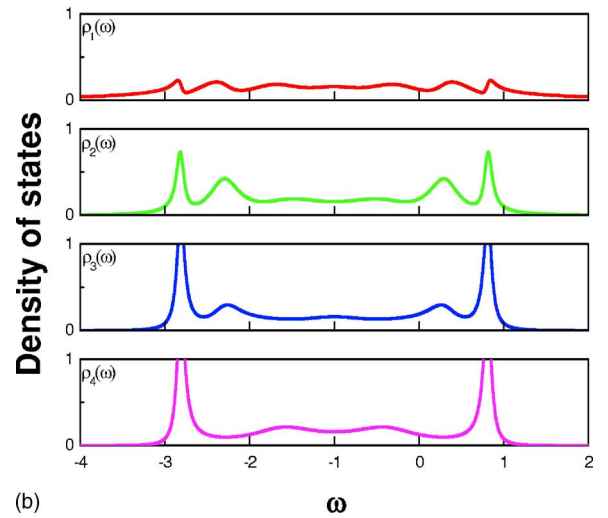


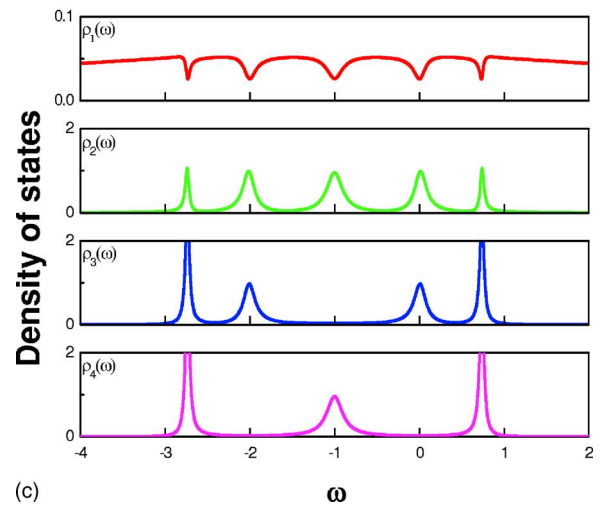
FIG. 2. (Color online) Plot of the differential conductance against the left Fermi level for $N=7$, $kT=0.08$, and $\varepsilon_0=-1$ at different resonant widths: $\Delta=0.1$ (green), 1.0 (red), 6.0 (blue). All energies are expressed by units of v .



(a)



(b)



(c)

FIG. 3. (Color online) Plot of the density of states of each dot in the quantum dot array for $N=7$, $\varepsilon_0=-1$, and different resonant widths: (a) $\Delta=0.1$; (b) $\Delta=1.0$; (c) $\Delta=6.0$. All energies are expressed by units of v . When $\Delta_L=\Delta_R$, we have $\rho_j=\rho_{N+1-j}$ for symmetry. That is, we have $\rho_1=\rho_7$ (red), $\rho_2=\rho_6$ (green), $\rho_3=\rho_5$ (blue), and ρ_4 (pink).

will be smoothed gradually and the “steps” in the dc current disappear eventually.

Figure 2 shows the dependence of the differential conductance on the bias voltage μ . At low temperatures, the differential conductance versus μ shows a multipeak structure when the resonant width Δ is much larger or smaller than the tunnel coupling v . Similar to the situation in the dc current, with increasing the temperature or the number of quantum dots, the multiple peaks in the differential conductance will become rounded gradually and eventually disappear.

Figures 1 and 2 exhibit an observable feature, that the ratio of the reservoir resonant width Δ to the interdot tunnel coupling v has a considerable effect on the dc current and the differential conductance. When the resonant width Δ is larger or smaller than the tunnel coupling v , the dc current and the differential conductance have small or intermediate values. Only for a special tunnel coupling can both the dc current and the differential conductance reach their extrema. In order to determine the optimal tunnel coupling relation in the dc current and the differential conductance, we investigate the area under the differential conductance curve with respect to μ . In terms of the exact formula for the differential conductance, the area under the differential conductance curve with respect to μ can be given by

$$\Gamma = \int d\mu \sigma(\mu) = \frac{4e^2}{h} \int d\omega \frac{\Delta^2}{[\eta^2(\omega) + \xi^2(\omega)]}. \quad (13)$$

We find that Γ is dependent only on the resonant width Δ and the interdot tunnel coupling v , but independent of the dot number and temperature. According to the extremum condition $\frac{\partial \Gamma}{\partial \Delta} = 0$, we have that for arbitrary QD number N

$$\Gamma_{\max} = \frac{\pi e^2}{h} \quad \text{when} \quad \frac{\Delta}{v} = 1.$$

This fact indicates that there exists an optimal tunnel coupling relation in the N -coupled quantum dot array. That is, when the interdot tunneling coupling v is equal to the reservoir resonant width Δ related to the tunnel coupling between the reservoir and its nearby quantum dot, the dc current and differential conductance reach their extrema.

Physically, this optimal tunnel coupling relation can be understood by the density of states of electrons in the quantum dot. Figure 3 shows the density of states of electrons in each dot. When Δ is smaller or larger than v [Figs. 3(a) and 3(c)], the density of states of electrons in each quantum dot shows the structure of the multiple energy levels. For the j th ($2 \leq j \leq N-1$) dot, the number of the oscillating peaks located in related energy levels is different from that in its neighboring ($j-1$)th and ($j+1$)th dots. This means that the positions and strengths of some energy levels in the j th dot are not in correspondence with that in ($j-1$)th and ($j+1$)th dots. This fact indicates that when the electrons oscillate among all the dots in the array, the tunneling effect among all the neighboring dots will be weakened. As a result, the current flowing through all the dots and the differential conductance will be diminished to some extent.

For the optimal tunnel coupling [Fig. 3(b)], however, the density of states of electrons in each quantum dot has been smoothed to the fullest extent and the electron energy levels become continuous. In this case, the tunneling effect among all the neighboring dots is strongest, meaning perfect transparency of the quantum dot array for transport. That is, most of the electrons from the right reservoir can pass easily through all the dots to the left reservoir. This, therefore, leads to the maximal dc current and differential conductance, as shown in Figs. 1 and 2.

In conclusion, we have calculated exactly the dc current, the differential conductance, and the density of states for the N -coupled quantum dot array. These analytically rigorous expressions for the quantum transport show explicitly algebraic structures. We have found that the dc current, the differential conductance and the density of states depend considerably on the ratio of the reservoir resonant width Δ to the interdot tunneling coupling v . When this resonant width Δ is equal to the tunneling coupling v , the density of states has been smoothed to the fullest extent. As a result, the dc current and differential conductance reach their extrema. Meanwhile for smaller quantum dots the dc current and the differential conductance exhibit respectively the steplike structure and the multi-peak resonant structure at low temperatures. In addition, these exact results may be used as a benchmark for numerical studies.

*Email address: phytbh@163.com (B. H. Teng).

¹C. Bruder and H. Schoeller, Phys. Rev. Lett. **72**, 1076 (1994).

²M. P. Anantram and S. Datta, Phys. Rev. B **51**, 7632 (1995).

³T. H. Oosterkamp *et al.*, Phys. Rev. Lett. **78**, 1536 (1997).

⁴L. P. Kouwenhoven *et al.*, Science **278**, 1788 (1997).

⁵G. Schedelbeck *et al.*, Science **278**, 1792 (1997).

⁶L. P. Kouwenhoven *et al.*, Rep. Prog. Phys. **64**, 701 (2001).

⁷J. M. Elzerman *et al.*, Nature (London) **430**, 431 (2004).

⁸R. Hanson *et al.*, Phys. Rev. Lett. **94**, 196802 (2005).

⁹E. Onac *et al.*, Phys. Rev. Lett. **96**, 176601 (2006).

¹⁰A.-P. Jauho *et al.*, Phys. Rev. B **50**, 5528 (1994).

¹¹T. Ivanov, Phys. Rev. B **56**, 12339 (1997).

¹²K. Kawamura and T. Aono, Jpn. J. Appl. Phys., Part 1 **36**, 3951 (1997).

¹³L. H. Lin *et al.*, Phys. Rev. B **60**, R16299 (1999).

¹⁴R. Ziegler *et al.*, Phys. Rev. B **62**, 1961 (2000).

¹⁵Z. Ma *et al.*, Phys. Rev. B **62**, 15352 (2000).

¹⁶W. Z. Shangguan *et al.*, Phys. Rev. B **63**, 235323 (2001).

¹⁷W. Lu *et al.*, Nature (London) **423**, 422 (2003).

¹⁸C. Flindt *et al.*, Phys. Rev. B **70**, 205334 (2004).

¹⁹W. G. van der Wiel *et al.*, Rev. Mod. Phys. **75**, 1 (2003).

²⁰B. Teng and H. K. Sy, Phys. Rev. B **70**, 104115 (2004).

²¹H. K. Sy, Phys. Rev. B **46**, 9220 (1992).